White Spot Syndrome Virus Open Reading Frame 222 Encodes a Viral E3 Ligase and Mediates Degradation of a Host Tumor Suppressor via Ubiquitination

Fang He,[1] Beau J. Fenner,[1] Andrew K. Godwin,[2] and Jimmy Kwang[1]*

Animal Health Biotechnology, Temasek Life Sciences Laboratory, National University of Singapore, Singapore 117604, Republic of Singapore,[1] and Department of Medical Oncology, Fox Chase Cancer Center, Philadelphia, Pennsylvania 19111[2]

We have characterized a white spot syndrome virus (WSSV) RING-H2-type protein, WSSV222, which is involved in ubiquitination. WSSV222 exhibits RING-H2-dependent E3 ligase activity in vitro in the presence of the specific conjugating enzyme UbcH6. Mutations in the RING-H2 domain abolished WSSV222-dependent ubiquitination, revealing the importance of this domain in WSSV222 function. Yeast two-hybrid and pull-down analyses revealed that WSSV222 interacts with a shrimp tumor suppressor-like protein (TSL) sharing 60% identity with human OVCA1. To better characterize the interaction of WSSV222 and TSL in vivo, we established a stable TSL-expressing cell line derived from the human ovarian cancer cell line A2780, where we observed a TSL-dependent prolonged G_1 phase. Furthermore, we detected WSSV222-mediated ubiquitination and MG132-sensitive degradation of TSL both in shrimp primary cell culture and in the TSL-expressing cell line. Transient expression of TSL in BHK cells leads to apoptosis, which was rescued by WSSV222. Taken together, our data suggest that WSSV222 acts as an antiapoptosis protein by ubiquitin-mediated proteolysis of TSL to ensure successful WSSV replication in shrimp.

White spot syndrome virus (WSSV) is a virulent shrimp pathogen responsible for high mortality in cultured shrimp, raising major concerns in the aquaculture industry. Disease outbreaks can reach a cumulative mortality of up to 100% within 3 to 7 days of infection (23). Its circular double-stranded DNA genome, one of the largest viral genomes, consists of 300 kbp that contain approximately 185 open reading frames (ORFs) (37, 43). Database searches reveal that more than 95% of these ORFs do not have any counterparts in other species, and WSSV has thus been placed in a new virus family, the *Nimaviridiae*, genus *Whispovirus* (37). So far, only a few non-structural genes from WSSV which show homology to known sequences in the databases have been identified and characterized; these include a ribonucleotide reductase (35) and a DNA polymerase (10). At the molecular level, there is little understanding of how WSSV establishes latent infections or of the genes responsible for the transition between latent and lytic infection, which eventually leads to mortality.

Ubiquitin-dependent proteolysis serves a central regulatory function in many biological processes, such as cell cycle regulation, signal transduction, and transcriptional regulation (4, 24, 45). Importantly, ubiquitin-mediated degradation of cellular tumor suppressors is essential for regulation of cell division and apoptosis, and many apoptosis-regulatory proteins have been identified as target substrates for ubiquitination (14, 45). For example, the intracellular level of p53 is mainly down-regulated by the RING-domain protein Mdm2 via an E3 ligase (13). It is therefore not surprising that many viruses possess their own E3 ligases, such as ICP0 from herpes simplex virus type 1 (5, 12) and E6AP from human papillomavirus (34), for ubiquitination and degradation of host tumor suppressors to achieve a quiescent cellular environment for virus replication (3, 38). In baculoviruses, the inhibitors of apoptosis proteins function as E3 ligases, and the number of identified cellular targets of this class of proteins, which includes caspases, is increasing (38).

The RING finger domain is found in the largest known class of E3 ubiquitin ligases (46). It has functions involved in cell-cycle control, oncogenesis, apoptosis, and the regulation of virus replication in the host (4, 18, 29). RING finger domains are subdivided into two subgroups, the C3HC4 (RING-HC) subgroup and the C3H2C3 (RING-H2) subgroup (4). Four proteins of WSSV, namely, WSSV199, WSSV222, WSSV249, and WSSV403, contain RING-H2-domains (41, 43). Among them, WSSV249, acting as an E3 ligase, sequesters the shrimp E2 ubiquitin-conjugating enzyme PvUbc for viral pathogenesis (41). Here, we focus on another candidate, WSSV222.

In this report, we show that WSSV222 functions as a RING-dependent E3 ligase. Yeast two-hybrid and pull-down analyses revealed that WSSV222 interacts with a shrimp tumor suppressor-like protein (TSL). The extensive identity shared by the human OVCA1 (ovarian cancer 1) tumor suppressor (9, 30) and TSL suggested a role for TSL in apoptosis regulation. Here, we show that TSL has a role in regulating the cell cycle and that WSSV222 inhibits apoptosis. Biochemical analyses show that WSSV222 can interact with and mediate the ubiquitination and degradation of TSL and that this effect represents a biologically significant balance between WSSV replication and cellular suicide.

* Corresponding author. Mailing address: Animal Health Biotechnology, Temasek Life Sciences Laboratory, 1 Research Link, National University of Singapore, Singapore 117604, Republic of Singapore. Phone: (65) 6872 7473. Fax: (65) 6872 7007. E-mail: kwang@tll.org.sg.

MATERIALS AND METHODS

Rapid amplification of cDNA ends (RACE) PCR and cloning of the wild type and mutants. Full-length WSSV222 and 222RING sequences ranging in size from 637 to 1,494 bp were amplified from viral DNA that had been extracted

previously (20) with primer pair 222f (5′-ATGTTCACTCACTTGACC-3′) and 222r (5′-TTAGATTAAAGTAAAACAGTACAT-3′) and primer pair 222RINGf (5′-CCTACTACTAGCCAACAC-3′) and 222RINGr (5′-GCGCATCTGTATTTGTCT-3′), respectively. WSSV222 mutations C311S, H336Y, and 307DEL347 were created using a QuickChange site-directed mutagenesis kit (Stratagene).

Forward (5′-GGCATACGATGGTGTGTCCCTCGGG-3′) and reverse (5′-GGGCTGGTCATAGTATTCACGGGAAAGGAC-3′) primers were designed to determine the transcription start site of shrimp TSL using a RLM-RACE kit (Ambion) according to the manufacturer's instructions. RACE products were ligated to pGEM-T Easy (Promega) and sequenced. Together with 3′ end sequence information from the original library insert sequencing, forward (5′-ATGAATATGGAGGAAGATACGCA-3′) and reverse (5′-ATCTTTATTACTTCCTTGTTTAGAGCT-3′) primers for the full-length TSL were designed to amplify the full-length TSL fragment.

Yeast two-hybrid assays. Two-hybrid assays were performed using a Matchmaker GAL4 kit (Clontech). Growth conditions, media, and transformation protocols were as described by the manufacturer. The bait construct pGBKT7-222 and the shrimp cDNA library in pGADT7 were used to cotransform yeast strain AH109. Transformants were selected for growth on medium lacking His, Leu, and Trip (−His/−Leu/−Trp). The selected colonies were then transferred to −Ade/−His/−Leu/−Trp plates containing 250 μl of X-α-Gal (5-bromo-4-chloro-3-indolyl-α-D-galactopyranoside; 2 mg/ml in N,N-dimethylformamid; Genomax) per 15-cm plate. Blue colonies were selected and cultured in −Ade/−His/−Leu/−Trp broth and lysed with glass beads (Sigma) for plasmid isolation in lysis buffer (2% Triton X-100, 1% sodium dodecyl sulfate [SDS], 100 mM NaCl, 10 mM Tris-HCl [pH 8.0], 1 mM EDTA). Isolated plasmids were amplified in *Escherichia coli* DH5α, and the target insertions were verified by sequencing. Target and bait plasmids were then cotransformed into AH109 to reconfirm the interactions.

Expression and purification of proteins and antibody preparation. Wild-type 222RING and its mutants were ligated to pQE30 (QIAGEN) using BamHI and SalI sites for construction of expression plasmids. Transformed *E. coli* M15 (pREP4) cells were cultured in LB medium with ampicillin (200 μg/ml) at 16°C and induced with 1 mM isopropyl-1-thio-β-D-galactopyranoside (IPTG). Full-length WSSV222 was expressed using a Bac-to-Bac system (Invitrogen) according to the manufacturer's instructions. Bacteria or SF9 cells were harvested by centrifugation, resuspended in lysis buffer with nickel-nitrilotriacetic acid beads, and lysed by sonication. The expressed proteins were then bound to nickel-nitrilotriacetic acid beads (New England BioLabs) and washed with buffers under native conditions. The purified protein-conjugated beads were then denatured in Laemmli sample buffer prior to SDS-polyacrylamide gel electrophoresis (PAGE) on a 12% gel. Proteins were electroblotted onto a polyvinylidene difluoride membrane followed by blocking in 5% bovine serum albumin. Blots were probed with a 1:2,000 dilution of mouse anti-His$_6$ (New England BioLabs) followed by a 1:2,000 dilution of horseradish peroxidase-conjugated rabbit anti-mouse immunoglobulin G (IgG; DAKO Cytomation) prior to development of the diaminobenzene substrate.

Plasmids pGEX4T-TSL and pGEX4T were transformed into *E. coli* DH5α. Cultures in LB medium with ampicillin were grown to mid-log phase at 37°C before being induced with 1 mM IPTG for 5 h at 25°C. Bacterial pellets were resuspended in phosphate-buffered saline (PBS), lysed by sonication, and clarified by centrifugation at 3,000 × g for 15 min. Glutathione S-transferase (GST)-TSL and GST proteins were bound to glutathione Sepharose 4B beads (Amersham) and eluted from beads in PBS containing 50 mM glutathione. The purified proteins were verified on 12% SDS-polyacrylamide gels by immunoblotting with an anti-GST antibody (Pierce).

Mice were boosted three times with the same quantities of antigen emulsion for TSL or WSSV222 every other day for 14 days. Ten days after the final booster injection, the animals were sacrificed by exsanguination and sera were collected.

Pull-down assays. Cell lysates from WSSV222 and mutant expression constructs were incubated with purified GST-TSL or GST protein (negative control) at 4°C for 4 h. The mixtures were clarified by centrifugation at 1,500 × g for 10 min, and the supernatants were precleared using fresh GST beads and then washed in ice-cold wash buffer (100 mM Tris-HCl [pH 8.0], 150 mM NaCl, 5% glycerol, 0.1% Nonidet P-40, 5 mM β-mercaptoethanol) five times at 4°C. The beads were then denatured in Laemmli sample buffer prior to SDS-PAGE and immunoblotting with anti-His$_6$ and anti-GST antibodies, respectively.

Cell culture, immunofluorescence, and confocal microscopy. Lymphoid organs were excised from adult *Penaeus vannamei*, separated into small fragments using sterilized forceps, and then incubated at 28°C in 2× L15 complete medium containing 20% fetal bovine serum (FBS). The original medium was removed with the unattached tissue after 12 h. The remaining cells were inoculated with WSSV in serum-free 2× L15 medium for 1 h and were then transferred into fresh complete medium (39). The cells were fixed with 100% ethanol at 24 h

postinoculation and then incubated with anti-TSL or anti-222 serum (1:50 dilution in PBS) and fluorescein isothiocyanate-conjugated anti-guinea pig IgG or anti-mouse IgG (1:50 dilution in PBS; DAKO) sequentially at 37°C. Finally, the cells were observed under a fluorescence microscope.

A2780 cells (Fox Chase Cancer Center) were grown in RPMI medium supplemented with 10% FBS and 0.33 IU/ml porcine insulin at 37°C. BHK (baby hamster kidney) cells were grown in Dulbecco modified Eagle medium supplemented with 10% FBS at 37°C. The cells were transfected with pWSSV222-EGFP, pTSL-EGFP, pcDNA-TSL, or vector (negative control) using Lipofectamine and Plus reagents (Invitrogen), as described by the manufacturer. Clones that stably expressed TSL were obtained after selection in G418 (GIBCO) by standard methods and maintained in RPMI supplemented with 10% FBS and 0.5 mg/ml G418. For degradation assays, the A2780 cells were treated with 30 μM MG132 (Boston Biochem) overnight to allow accumulation of TSL. Cells (10^6) were suspended into a final volume of 200 μl. Twenty micrograms of total protein was loaded to SDS-PAGE from each sample. For microscopy, the cells were fixed at different stages by 4% PFA. The primary antibody used was anti-TSL guinea pig serum. The secondary antibody was rhodamine-conjugated rabbit anti-guinea pig IgG (Chemicon). Nuclei were stained with DAPI (4′,6′-diamidino-2-phenylindole; Invitrogen) and fluorescence observed with a confocal inverted laser microscope (Zeiss) with excitation recorded at 568 nm (red), 488 nm (green), or 420 nm (blue) (see Fig. 4A and 6A). Channels were recorded independently to avoid cross talk between the channels.

Ubiquitination assays in vitro and in vivo. E1 and E2 enzymes used in this experiment were purchased from Boston Biochem. In vitro ubiquitin conjugation assays were performed with a buffer containing 50 mM Tris-HCl (pH 7.5), 5 mM MgCl, and 2 mM ATP. The concentrations or amounts of proteins and enzymes used were as follows: 50 nM E1, 250 nM E2, 5 μg of ubiquitin (Sigma), approximately 200 ng of WSSV222, 222RING, C310S, H336Y, and Δ307/347, and 200 ng of TSL. For in vivo ubiquitination assays, total protein was extracted from TSL-expressing A2780 cells previously transfected with plasmids containing EGFP-222 or EGFP or from shrimp primary cells in the presence of protease inhibitor (Roche). Proteins were collected by sequential incubation of cell extracts with the appropriate antibody and protein A beads (Clontech). After a 4-h incubation at 30°C, the reactions were quenched with Laemmli sample buffer and subjected to electrophoresis on a 10% SDS-polyacrylamide gel. Proteins were transferred to a nitrocellulose membrane for immunoblotting and then probed sequentially using anti-ubiquitin monoclonal antibody P4D1 (1:1,000; Santa Cruz Biotechnology) and horseradish peroxidase-conjugated rabbit anti-mouse IgG (1:1,000) for in vitro assays and anti-TSL (1:1,000) and rabbit anti-guinea pig (1:1,000) IgG for in vivo assays. Bound antibody was detected using enhanced chemiluminescence reagent (Pierce) and exposure on film.

DNA fragmentation assays. BHK cells were transfected by electroporation with a Gene Pulser (Bio-Rad) using the preset BHK program. Low-molecular-weight DNA was isolated from transfected cells with an apoptotic DNA ladder kit (Roche) according to the manufacturer's instructions. Equal amounts of DNA were resolved on a 1% agarose gel containing ethidium bromide.

Fluorescence-activated cell sorter (FACS) analysis. Cells were harvested, washed with PBS, and fixed with 75% ethanol at room temperature for 30 min, followed by treatment with 10 μg/ml RNase at 37°C for 30 min. Nuclei were stained with 50 μg/ml propidium iodide (Clontech) for 30 min. The cells were filtered through a 40-μm nylon mesh and then analyzed by flow cytometry (BD Immunocytometry Systems). Data for 10,000 events were gathered by CellQuest software (BD Immunocytometry Systems) and analyzed using FCS Express version 3.

RESULTS

WSSV222 is a RING-H2 E3 ligase. An initial characterization of the putative protein encoded by WSSV ORF222 revealed the presence of a RING finger domain (26) similar to those from mammals and viruses (Fig. 1A). The presence of a C3H2C3-type RING finger suggested that WSSV222 belongs to the RING-H2 subgroup and could be involved in protein-protein interactions.

To focus on the RING domain function of WSSV222, we constructed and expressed a partial WSSV222 protein, termed 222RING, which contains the RING finger domain (P212–R498) (Fig. 1B). E3 ligases are known to specifically stimulate
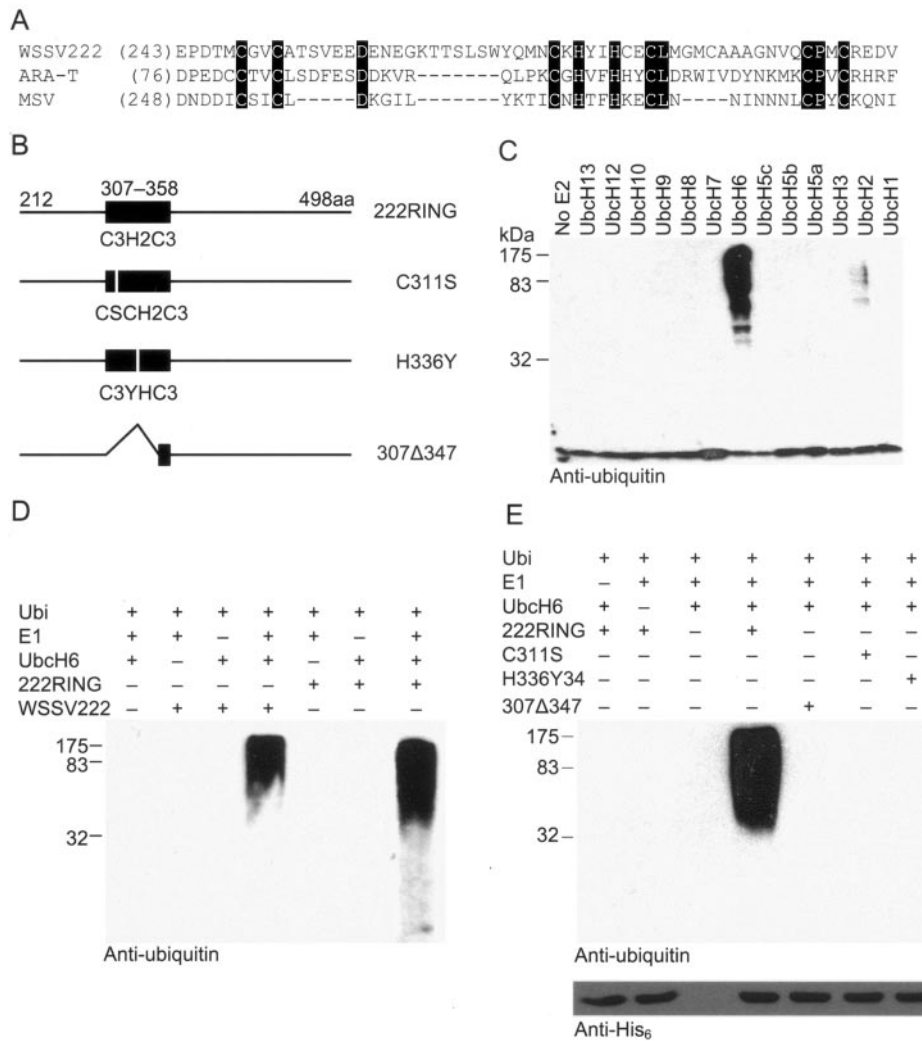
FIG. 1. WSSV222 is a RING-containing E3 ligase. (A) Sequence alignment of the N-terminal portion WSSV222 with related proteins. The WSSV222 RING domain is of the C3H2C3 type ($CX_2CX_{9-39}CXHX_2HX_2CX_{4-48}CX_2C$), similar to that of *Arabidopsis* (ARA-T) and ORF MSV251 (*Melanoplus sanguinipes* entomopoxvirus; MSV). Black highlights consensus residues for RING structure among the three species. (B) Schematic representation of WSSV222 protein and mutant constructs. (C) In vitro conjugation assay using anti-ubiquitin antibody P4D1, as described in Materials and Methods. A panel of different E2 enzymes was screened for activity in the presence of 222RING. The negative control reaction was performed in the absence of E2 (No E2). (D) Both full-length WSSV222 and RING domain of WSSV222 have polyubiquitination activity under a specific E2 enzyme, UbcH6. The negative control reaction was performed in the absence of E1 or E2. (E) Effects of mutations in WSSV222 on the in vitro conjugation reaction. Purified mutant and wild-type 222RING proteins were subjected to an in vitro ubiquitination assay using E1, UbcH6, and ubiquitin. The input amount of E3 ligase was the same, detected by anti-His$_6$ antibody. Ubi, ubiquitin.

E2-conjugating enzymes based on their specific interaction with the E3 ligase RING finger domain of E3 (18, 19). To determine if WSSV222 possessed ubiquitination activity in vitro and which, if any, E2 enzyme stimulated this activity, we incubated purified 222RING with a range of different E2 enzymes in the presence of all the other components in an in vitro ubiquitination assay. E3 ligase activity of 222RING was strongly stimulated only by UbcH6, while the other E2 enzymes tested showed no stimulation in spite of their normal conjugating activity (Fig. 1C). Among these, the activation of E2, UbcH1, H2, H3, H5a, H5b, H5c, H6, H9, and H10 has been reported previously by our laboratory (41), while UbcH7, H8, H12, and H13 were incorporated into the study but did not stimulate 222RING activity. Based on this observation, we

introduced full-length WSSV222 to the assay. Full-length WSSV222 and 222RING autoubiquitinated in the presence of the other components, including UbcH6 (Fig. 1D). This result indicated that WSSV222 is indeed an E3 ligase and that it specifically recognizes UbcH6, resulting in autoubiquitination. The 222RING fragment, which covers a complete RING-H2 domain, is sufficient and independent to support such E3 ligase activity.

To further investigate the RING domain function of WSSV222, we prepared a number of mutant derivatives of 222RING (Fig. 1B). C311S and H336Y are WSSV222 RING finger mutants with an altered C3H2C3 RING finger structure and are thus unable to bind monovalent zinc ions, which are required for E3 ligase activity (4). Mutant 307Δ347 lacks most

A

```
TSL protein    ----MNMEEDTQSKEIVVAPKKEKKVFRPARSVIKGVPAEIEKDPKLQKAIEVLPSNYNFEIPKTIWRVKQANAKHVALQ
Human OVCA1    MRRQVMAVLVVSGAAEQGGRDGPGRGRAPRGRVANQIPPEILKNPQLQAAIRVLPSNYNFEIPKTIWRIQQAQAKKVALQ
Mouse OVCA1    -----MAALVVSETAEPGSRVGPGRGRISRGRLANQIPPEVLNNPQLQAAVQVLPSNYNFEIPKTIWRIQQAQAKKVALQ
Cons                 ..        .      .    : : :*.*: ::*:** *:.***************:::**:**:****

TSL protein    FPEGLLLFATSIADIIETWTEAETTIMGDVTYGACCVDDFTARAVGADFMVYHGHSCLVPIDQTGS-IPCLYVFVDIQFD
Human OVCA1    MPEGLLLFACTIVDILERFTEAEVMVMGDVTYGACCVDDFTARALGADFLVYHGHSCLIPMDTSAQDFRVLYVFVDIRID
Mouse OVCA1    MPEGLLLFACTIVDILERFTEAKVMVMGDVTYGACCVDDFTARALGVDFLVYHGHSCLVPMDTSVQDFRVLYVFVDIRID
Cons           :*******  :*.**:* :***:. :*****************:*.**:********:*:*  : .:  *******::*

TSL protein    TVHLIDTIKSVFPSTVPLALVSIIQFVSSLQKMAQDLKSCGYTVCVPQCRPLSPGEVLGCTSPPVP-EGHTIVCLGDGRF
Human OVCA1    TTHLLDSLRLTFPPATALALVSTIQFVSTLQAAAAQELKA-EYRVSVPQCKPLSPGEILGCTSPRLSKEVEAVVYLGDGRF
Mouse OVCA1    TAHLLDSVRLTFTPGSSLALVSTIQFVSTLQAAAAQELKA-DYHISVPQCKPLSLGEILGCTSPRLSKEVEAVVYLGDGRF
Cons           *.**:*::: .*..  .***** *****:**  **:**:  * :.****:*** **:****** :. *  .::* ******

TSL protein    HLESIMISNPEVPTYLYNPYSKVLSREYYDQPLMKKIRKEIIDKASTAKKWGLILGTLGRQGNTKVMENLKNQLEAAGKD
Human OVCA1    HLESVMIANPNVPAYRYDPYSKVLSREHYDHQRMQAARQEAIATARSAKSWGLILGTLGRQGSPKILEHLESRLRALGLS
Mouse OVCA1    HLESVMIANPNIPAYRYDPYGKVLSREYYDHQRMQATRQEAIAAARSAKSWGLILGTLGRQGSPKILEHLESQLRNLGLP
Cons           ****:**:**::*:* *:**.******:**: *:  *:* *   * :**.************..*::*:*:.:*.  *

TSL protein    FVIVLLSEIFPAKLEAMSDVEAWVQVACPRLSIDWGASFPRPLLNPYEATVALKHAEWHAQRYPMDFYANESLGEWTPNH
Human OVCA1    FVRLLLSEIFPSKLSLLPEVDVWVQVACPRLSIDWGTAFPKPLLTPYEAAVALRDISWQ-QPYPMDFYAGSSLGPWTVNH
Mouse OVCA1    FVRLLLPEIFPSKLSLLPEVDVWVQVACPRLSIDWGSAFPKPLLTPYEAAVALKDISWQ-QPYPMDFYSGSSLGPWTVNY
Cons           ** :**.****:**. .::*:*.************:***:.* ***.**** :**:***.  .*: * ******:..*** ** *:

TSL protein    -KPPCPCGQTRNT--------------GCKGLRCPSSKQGSNKD
Human OVCA1    GQDRRPHAPGRPARGKVQEGSARPPSAVACEDCSCRDEKVAPLAP
Mouse OVCA1    GRDRAPRGLCQPASDKVQQGSRGGSPAPACESCNCADQKATSPAP
Cons           : ::: ::   ::  ::   :    : .*:. * ..* . ::
```

B

C

D

FIG. 2. Shrimp TSL is functionally similar to human OVCA1. (A) Amino acid sequence alignment of the shrimp TSL and related proteins. TSL is 60% and 58% homologous to the human and mouse OVCA1 proteins, respectively. Cons, conserved; ., similar; :, highly similar; *, identical. (B) Flow cytometry analysis of TSL-expressing A2780 cells. Cell cycle distributions were determined at 24 h postseeding by FACS. DNA profiles represent cell number (Events) along the ordinate and DNA content along the abscissa. The percentages of cells in the G_1 and G_2 phases of the cell cycle are listed. A2780, original cells; Vector, vector control; TSLA and TSLB, TSL-expressing cell lines from colonies A and B, respectively. (C) Immunoblot showing exogenous TSL expression in TSL-expressing A2780 cells detected in different clones with anti-TSL antibody. (D) TSL localization in A2780 cells with TSL clone A. TSL-expressing A2780 cells were fixed at 24 h postseeding and stained with anti-TSL antibody. Control, original A2780 cells.

of the RING finger domain, thereby abolishing its ubiquitination function. Expressed proteins were verified by immunoblotting using anti-His$_6$ (Fig. 1E). Wild-type 222RING and mutant proteins were then included in ubiquitination assays, and the reactions were analyzed by immunoblotting using monoclonal anti-ubiquitin antibody to detect E3 ligase activities in vitro. Only the wild-type 222RING protein showed a ladder-like smear with high-molecular-weight proteins, a result which can be attributed to polyubiquitin chains in the presence

of E1, UbcH6, and ubiquitin (Fig. 1E). In contrast, none of the mutated RING finger proteins showed polyubiquitination activity with the same input amount of E3 (Fig. 1E). These results indicate that the intact RING domain in WSSV222 is both necessary and sufficient for its E3 ligase function.

TSL, a shrimp orthologue for OVCA1, is a WSSV222 target. To elucidate the function of the RING domain in WSSV222 and the significance of its E3 ligase function for WSSV infection, we investigated the protein-protein interactions between

the virus and its host using a yeast two-hybrid system. From these assays, a putative WSSV222 partner was identified. The amino acid sequence of this construct has high similarity to the human tumor suppressor *OVCA1* (ovary cancer gene 1). *OVCA1* is expressed ubiquitously in human tissues and mammalian cell lines to various degrees (17), and its expression inhibits tumor growth in vivo and in vitro (7). The sequence obtained by yeast two-hybrid assay from the shrimp cDNA library is shorter than OVCA1 and apparently lacked the N-terminal region. The complete sequence with a Kozak consensus start codon was determined from shrimp cDNA by 5′ RACE and was named shrimp TSL. The full-length shrimp TSL (AAU13908) was predicted to be 1,272 bp, and the encoded protein shares 60% and 59% amino acid sequence identity with human and mouse OVCA1, respectively (Fig. 2A). There is no conserved motif or known functional domain in shrimp TSL or mammalian OVCA1. To further understand the function of shrimp TSL, we established a TSL-expressing cell line in the A2780 human ovarian cancer cell line. Expression of TSL in these cells was confirmed from several clones by immunoblotting with an anti-TSL antibody, although expression levels varied somewhat (Fig. 2C). FACS assays with either clone A or clone B also indicated that TSL is expressed in A2780 cells and that it suppressed cell growth at the G_1 phase: a 15 to 17% increase in the number of cells in G_1 phase was observed for these cells compared with a vector-transformed control (Fig. 2B). This cell cycle-regulating property of TSL closely resembles the activity of human OVCA1 (27). TSL was localized throughout the cell from TSL clone A but mainly in the cytoplasm (Fig. 2D), which corresponds to the localization pattern of human OVCA1 (7). Taken together, these data indicate that shrimp TSL is an orthologue of human OVCA1 and an interaction partner of WSSV222.

WSSV222 interacts with and ubiquitinates TSL in vitro. To further confirm the interaction between TSL and WSSV222, GST pull-down assays comparing shrimp TSL and WSSV222 were performed (Fig. 3A). GST-TSL, but not GST, interacted with full-length WSSV222 from a total cell lysate, thus forming soluble complexes that could be isolated by glutathione Sepharose. His$_6$-tagged WSSV222 was detected by anti-His$_6$ antibody in the GST-TSL sample but was clearly absent in the GST control (Fig. 3A). Meanwhile, both TSL-GST and GST could be detected by anti-GST antibody, showing bands corresponding to their respective molecular weights. Experiments performed with 222RING and its mutants revealed that all of the proteins specifically interacted with GST-TSL but not with GST, indicating that an intact RING domain is not essential for protein binding and that 222RING includes a TSL interaction domain other than the RING domain. Immunoblot data confirmed the strong protein-protein interaction between shrimp TSL and WSSV222 as observed from yeast two-hybrid assays, whereby yeast colonies cotransformed with either shrimp TSL and full-length WSSV222 or shrimp TSL and 222RING grew under high stringency conditions (data not shown).

E3 ligases interact with several different components, such as E2 enzymes and substrates, for ubiquitination (18). To determine the role that TSL plays for WSSV222, we included purified GST-TSL in our polyubiquitination reaction. In the presence of all components, including WSSV222 as an E3
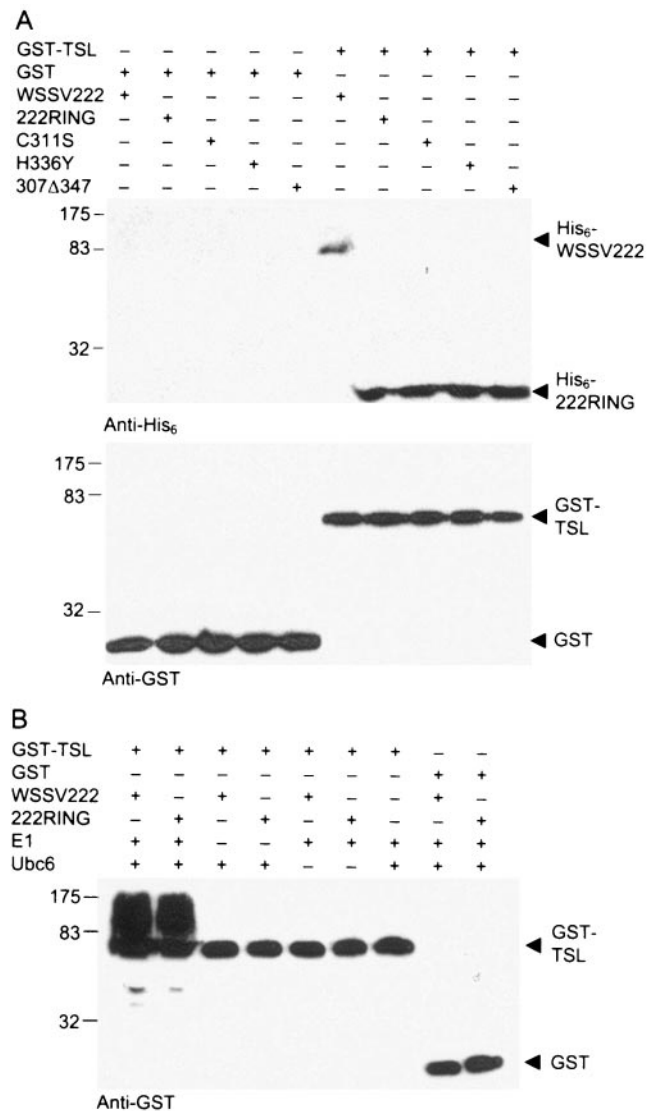

FIG. 3. WSSV222 interacts with and ubiquitinates shrimp TSL in vitro. (A) A His$_6$-WSSV222 pull-down assay was performed using soluble extracts of *E. coli* or SF9-expressed WSSV222 mixed with GST-TSL. Soluble protein complexes were bound to GST beads and washed under high stringency condition before SDS-PAGE and immunoblot detection of His$_6$-WSSV222 and 222RING. Immunoblots were performed with anti-His$_6$ or anti-GST. (B) In vitro polyubiquitination assay performed using WSSV222 and 222RING with TSL in the presence of E1, E2, and ubiquitin. SDS-PAGE-resolved complexes were immunoblotted with anti-GST antibody. The negative control reaction was performed in the absence of E1 or E2 or with GST instead.

ligase, GST-TSL was polyubiquitinated, as indicated by a high-molecular-weight smear (Fig. 3B). This strong signal was detected by anti-GST but was absent in the GST control. Polyubiquitination also was eliminated when WSSV222 was not included in the assay. In these experiments, GST was used as a tag to identify the polyubiquitin signal but not ubiquitin, indicating that this assay is specific for polyubiquitin signals generated from ubiquitinated substrate rather than from WSSV222 E3 ligase. These data indicate that TSL is a sub-
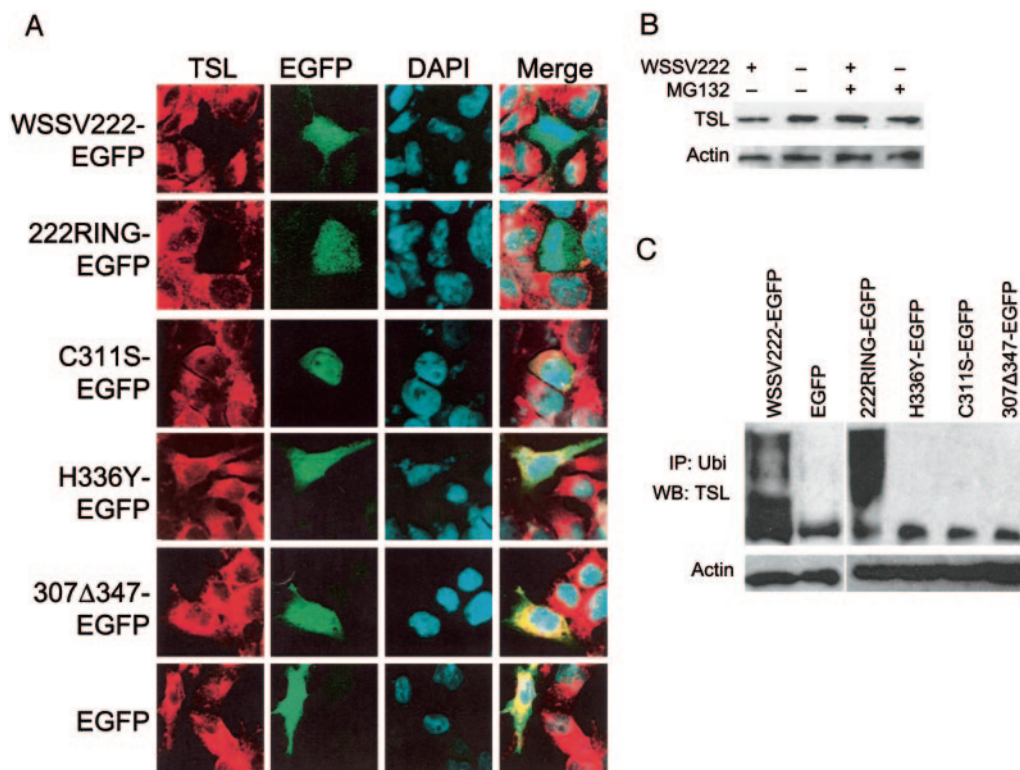
FIG. 4. WSSV222 ubiquitinates and mediates degradation of shrimp TSL in vivo. (A) Localization of WSSV222 and TSL in A2780 cells (TSL clone A). TSL-expressing A2780 cells were transfected with pWSSV222-EGFP (WSSV222-EGFP), p222RING-EGFP (222RING-EGFP) and its mutants, or pEGFP (EGFP). At 24 h posttransfection, cells were fixed and stained with anti-TSL antibody and rhodamine anti-guinea pig. Note the absence of TSL expression in cells containing WSSV222-EGFP and 222RING-EGFP. (B) Degradation of TSL by WSSV222 detected by immunoblotting with extracts from TSL-expressing A2780 cells harvested at 24 h posttransfection. TSL expression is recovered by MG132 treatment. (C) In vivo polyubiquitination of TSL. Cell lysates were prepared from TSL-expressing A2780 cells 24 h after transfection with pWSSV222-EGFP, p222RING-EGFP and its mutants, or pEGFP and subjected to immunoprecipitation with anti-ubiquitin antibody from mouse. Proteins were analyzed by immunoblotting with anti-TSL antibody from guinea pig. IP, immunoprecipitation; Ubi, ubiquitin; WB, Western blot.

strate for the WSSV222 E3 ligase for polyubiquitination in vitro. A similar result was observed in the same test with 222RING but not with any of the WSSV222 RING mutants. This result confirmed that substrate ubiquitination depended on E3 ligase activity and that the E3 ligase activity of WSSV222 depends on a complete and functional RING domain.

TSL is ubiquitinated for degradation by WSSV222 in vivo. To test whether TSL is also ubiquitinated in vivo, we performed ubiquitination assays using A2780 cells. Thus, TSL-expressing A2780 cells (TSL clone A) were transfected with pWSSV222-EGFP or pEGFP. Total protein extracted at 24 h posttransfection was incubated with anti-ubiquitin antibody and protein A beads. TSL protein was then immunoprecipitated and analyzed by immunoblotting with anti-TSL primary antibody. TSL precipitated from the pWSSV222-EGFP-transfected cell was polyubiquitinated, giving a high-molecule-weight smear, while the sample from the pEGFP control did not (Fig. 4C). We also performed such tests with 222RING and its mutants. As expected from our in vitro results, 222RING expression, but not that of the RING mutants, resulted in the ubiquitination of TSL (Fig. 4C), confirming that ubiquitination of TSL depends on the RING domain of the WSSV222 E3 ligase. To further clarify the fate of TSL ubiquitinated by WSSV222, we transfected TSL-expressing A2780 cells with

pWSSV222-EGFP or pEGFP and subjected the cells to an indirect immunofluorescence assay with anti-TSL antibody. We observed by confocal microscopy that cells transfected with EGFP-222 failed to yield a TSL-specific signal (Fig. 4A). Degradation of TSL was also detected in the presence of 222RING but not with the RING mutants, further verifying that degradation of TSL is mediated by E3 ligase-dependent ubiquitination.

We next sought to determine if TSL was being degraded via the 26S proteasome pathway, as would be expected for ubiquitin-mediated proteolysis. To accomplish this, we treated one set of transfected cells with MG132, a 26S proteasome inhibitor, and subjected the transfected cells to immunoblotting with anti-TSL antibody. We observed a decrease in the amount of TSL expressed in cells cotransfected with pWSSV222-EGFP and recovery by MG132 treatment, indicating that WSSV222 can degrade shrimp TSL via the 26S proteasome pathway. In the absence of WSSV222 expression, no obvious change in TSL expression level was detected in the TSL-expressing cell line treated with MG132 compared with original TSL cells (Fig. 4B). Therefore, the TSL recovered following MG132 treatment is specifically involved in WSSV222 pathway.

TSL is subjected to ubiquitination and degradation in WSSV-infected shrimp cells. To investigate the interactions between WSSV222 and shrimp TSL during WSSV infection,
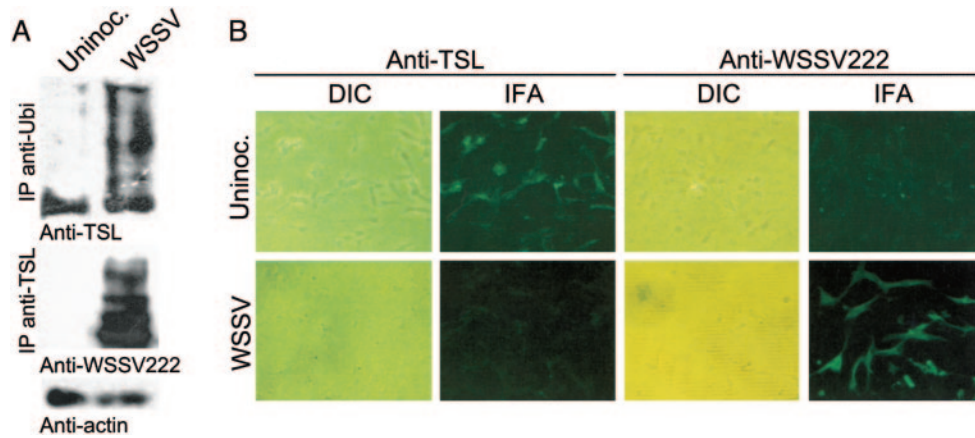
FIG. 5. TSL is degraded and ubiquitinated in WSSV-infected shrimp cells. (A) Coimmunoprecipitation and immunoblotting with total protein lysate from shrimp primary cells at 24 h postinoculation in the presence of 5 μM MG132. (B) Immunofluorescence assays with shrimp primary cells. Cells were fixed at 24 h postinoculation and stained with anti-TSL and anti-WSSV222 antibodies, respectively. Uninoculated cells are controls. IP, immunoprecipitation; Uninoc., uninoculated cells; WSSV, WSSV-inoculated cells; DIC, differential interference contrast; IFA, immunofluorescence assays by fluorescence microscopy (original magnification, ×200).

we performed immunofluorescence assays with shrimp primary cells. WSSV222 expression was detected with anti-WSSV222 among primary cells at 24 h postinoculation but not in uninoculated cells based on anti-WSSV222 fluorescence signals. Fluorescence from TSL was weaker in infected cells than in uninfected ones, suggesting degradation of TSL after WSSV infection (Fig. 5B). Coimmunoprecipitations using infected and uninfected cell lysates incubated with 5 μM MG132 showed that TSL from the infected lysate was polyubiquitinated, while that in the uninfected lysate was not (Fig. 5A). WSSV222 was detected in the lysate precipitated by anti-TSL antibody (Fig. 5A), verifying the interaction between WSSV222 and TSL in shrimp tissue culture. Moreover, the recovered WSSV222 was polyubiquitinated, clearly showing that it functions as an E3 ligase in shrimp cells. These results confirm the role of WSSV222 as a viral E3 ligase mediating

ubiquitination and subsequent degradation of shrimp TSL in WSSV-infected shrimp.

WSSV222 rescues apoptosis induced by transient expression of TSL in BHK cells. The nature of WSSV222-mediated TSL degradation in vivo was investigated by transiently expressing both TSL and WSSV222 in BHK cells. Membrane blebbing and DNA fragmentation were observed for TSL-expressing cells, while cells transfected with the EGFP parent vector still appeared healthy, as revealed by confocal microscopy (Fig. 6A). Additionally, DNA extracted from TSL-expressing cells at 24 and 48 h exhibited clear fragmentation (Fig. 6B), indicating cell apoptosis induced by TSL transient expression. This DNA fragmentation was rescued by cotransfection with pWSSV222-EGFP but not with the pEGFP control (Fig. 6C), indicating that WSSV222 can inhibit the apoptosis induced by TSL overexpression. Apoptotic blebbing in TSL-
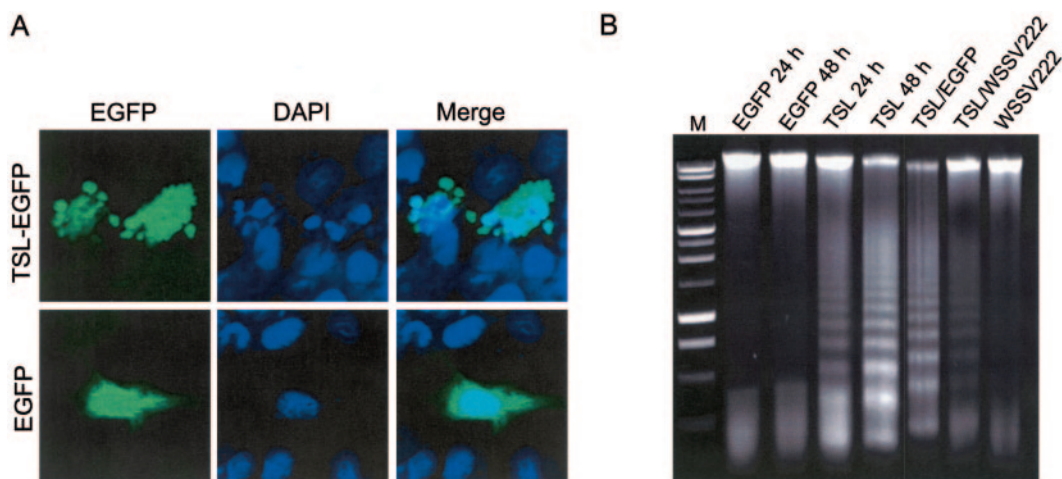

FIG. 6. WSSV222 antagonizes TSL-induced apoptosis in BHK cells. (A) Apoptotic blebbing of TSL-expressing BHK cells. Cells were transfected with pTSL-EGFP (TSL-EGFP) or pEGFP (EGFP) and fixed at 24 h posttransfection. (B) DNA fragmentation analysis. DNA was extracted from transfected BHK cells at 24 or 48 h posttransfection and subjected to agarose gel electrophoresis. DNA fragmentation is evidenced by laddering of the smear. M, markers.

expressing A2780 cells was not observed (data not shown), suggesting that components of the apoptotic pathway for this cell line are compromised.

DISCUSSION

This is one of the first reports that sheds light on the molecular mechanism of WSSV infection and reveals a link between infection and host protein degradation. During virus infection, the targeting of cellular proteins for proteasomal degradation via ubiquitination is an important aspect of virus survival and replication (3, 11, 25, 27). Among them, cellular tumor suppressors are the main targets of many E3 ligases for the purpose of cell survival and transformation, because they can induce apoptosis in infected cells to restrict infection (3, 13, 34, 38). Here, we have identified an E3 ubiquitin ligase, WSSV222, from WSSV and also its cellular substrate, a shrimp tumor suppressor-like protein. Our data suggest that the proteolytic pathway in which WSSV222 and TSL are involved may serve as an antiapoptotic mechanism in host cells to ensure WSSV replication.

The number of potential E3 ligases present in sequence databases has been increasing rapidly in recent years (14). In this study, we have shown that WSSV222 is a genuine E3 ubiquitin protein ligase from WSSV that can specifically interact with an E2-conjugating enzyme and mediate transfer of ubiquitin to a specific substrate protein. The specificity displayed by WSSV222 may be attributed to its recognition of the extra C-terminal extension or tail of the core domain of UbcH6, which is a unique characteristic for Class II E2 enzymes (21). Three WSSV222 mutants with mutations or deletions in the RING-H2 domain fail to catalyze ubiquitination, thus confirming that the E3 ligase activity of WSSV222 is dependent on the RING structure. Moreover, mutations in the RING structure do not affect interaction between WSSV222 and TSL, confirming that this domain is not involved in substrate binding. That the 222RING fragment of WSSV222 autoubiquitinates and binds TSL clearly indicates that this region contains the E3 ligase function of WSSV222. More work is required to identify the exact binding site for substrates and bring a better understanding to this viral E3 ligase.

To date, no stable and transfectable shrimp cell line has been established. Moreover, efficient expression of certain genes in shrimp primary cells has not been achieved by groups working on WSSV. Therefore, we have instead used human A2780 cells here to investigate aspects of the TSL-WSSV222 interaction. According to previous study, A2780 cells (human ovarian cancer cells) are one of the only cell lines for successful stable expression of OVCA1, suggesting that overexpression of OVCA1 either blocks growth or is toxic to the cells (7). From data presented here, it is clear that OVCA1 and TSL share functional similarity in human and shrimp cells and that TSL is able to function effectively in a mammalian background. Most importantly, to clarify the roles of WSSV222 and TSL during WSSV infection, we further verified these results in shrimp primary cells (16, 39) by confocal microscopy and immunoprecipitation, proving that WSSV222 is a viral E3 ligase and that TSL is ubiquitinated and degraded after WSSV infection.

The identified ubiquitination target of WSSV222, termed TSL, shares 60% homology with human OVCA1, which is a tumor suppressor associated with ovarian carcinoma and which regulates cell proliferation and tumorigenesis (7–9, 17, 30). OVCA1, when stably expressed in the ovarian carcinoma cell line used here, induces a 10 to 20% increase in the proportion of cells in the G_1 phase (27). Consistent with these results, stable TSL expression induced a 16% increase in cells present in the G_1 phase, indicating that shrimp TSL and OVCA1 have similar functions in cell cycle regulation. TSL expression in A2780 cells still permitted cell growth, though the rate of growth was somewhat reduced. A prolonged G_1 phase was exhibited, quite similar to the situation with OVCA1-expressing A2780 cells (7). The precise role of OVCA1 in human tumor suppression remains unclear, though further work in our laboratory on TSL and WSSV222 function may well contribute to a better understanding of its role in human ovarian cancer in addition to furthering our knowledge of WSSV infection.

A degree of biological relevance of the TSL-WSSV222 interaction was established, showing that WSSV222 functions as an antiapoptotic protein. TSL can induce apoptosis in BHK cells, confirming its tumor suppressor function in mammalian cells. BHK cells are widely used for apoptosis studies (31, 33, 36) and retain many molecular components of the apoptosis cascade (1). Moreover, this tumor suppressor effect was antagonized by WSSV222, which highlights the role of WSSV222 as a viral antiapoptotic protein. These findings have implications not only for WSSV but also for the potential role of human OVCA1. Preliminary yeast two-hybrid assay data indicate that TSL also interacts with other proteins similar to mammalian proapoptotic and antiapoptotic regulators, such as prohibitin (15, 40), a potential tumor suppressor associated with breast cancer, and cathepsin B (28, 32), a cysteine protease with elevated expression in different cancer tissues and cells. All these data are indicative of TSL's role as a regulator of apoptosis and tumor suppression. WSSV infection results in apoptosis in shrimp cells (42), and the present work suggests that TSL may play an essential role in this process. Meanwhile, the present work implies that WSSV222 appears to be employed strategically by WSSV to inhibit such a tumor suppressor in host.

Ubiquitination of tumor suppressors is important for different kinds of cellular regulation (44, 45). In addition to polyubiquitination, monoubiquitination is involved in in vivo modification of tumor suppressors, such as p53 (2, 6, 22). In our studies, without WSSV222 or 222RING, cellular TSL protein was precipitated by anti-ubiquitin antibody, although no polyubiquitination signal was detected (Fig. 4D and 5A), implying that a part of TSL may be monoubiquitinated in vivo and regulated by ubiquitination machinery other than WSSV222.

In our study, we have characterized WSSV222 function as an E3 ubiquitin ligase and identified a tumor suppressor-like protein, TSL, from shrimp as a substrate for WSSV222. Upon interacting with WSSV222, shrimp TSL is ubiquitinated and degraded via the 26S proteasome. These reactions serve as an antiapoptotic process to favor host cell survival and WSSV replication. This finding elucidates one of the first-described WSSV infection mechanisms and thus improves our understanding of how this unique virus functions.

REFERENCES

1. **Arden, N., and M. J. Betenbaugh.** 2004. Life and death in mammalian cell culture: strategies for apoptosis inhibition. Trends Biotechnol. **22:**174–180.
2. **Asher, G., and Y. Shaul.** 2005. p53 proteasomal degradation: poly-ubiquitination is not the whole story. Cell Cycle **4:**1015–1018.
3. **Banks, L., D. Pim, and M. Thomas.** 2003. Viruses and the 26S proteasome: hacking into destruction. Trends Biochem. Sci. **28:**452–459.
4. **Borden, K. L.** 2000. RING domains: master builders of molecular scaffolds? J. Mol. Biol. **295:**1103–1112.
5. **Boutell, C., and R. D. Everett.** 2003. The herpes simplex virus type 1 (HSV-1) regulatory protein ICP0 interacts with and ubiquitinates p53. J. Biol. Chem. **278:**36596–36602.
6. **Brooks, C. L., M. Li, and W. Gu.** 2004. Monoubiquitination: the signal for p53 nuclear export? Cell Cycle **3:**436–438.
7. **Bruening, W., A. H. Prowse, D. C. Schultz, M. Holgado-Madruga, A. Wong, and A. K. Godwin.** 1999. Expression of OVCA1, a candidate tumor suppressor, is reduced in tumors and inhibits growth of ovarian cancer cells. Cancer Res. **59:**4973–4983.
8. **Chen, C. M., and R. R. Behringer.** 2004. Ovca1 regulates cell proliferation, embryonic development, and tumorigenesis. Genes Dev. **18:**320–332.
9. **Chen, C. M., and R. R. Behringer.** 2005. OVCA1: tumor suppressor gene. Curr. Opin. Genet. Dev. **15:**49–54.
10. **Chen, L. L., H. C. Wang, C. J. Huang, S. E. Peng, Y. G. Chen, S. J. Lin, W. Y. Chen, C. F. Dai, H. T. Yu, C. H. Wang, C. F. Lo, and G. H. Kou.** 2002. Transcriptional analysis of the DNA polymerase gene of shrimp white spot syndrome virus. Virology **301:**136–147.
11. **Coscoy, L., and D. Ganem.** 2003. PHD domains and E3 ubiquitin ligases: viruses make the connection. Trends Cell Biol. **13:**7–12.
12. **Everett, R. D.** 1999. A surprising role for the proteasome in the regulation of herpesvirus infection. Trends Biochem. Sci. **24:**293–295.
13. **Fang, S., J. P. Jensen, R. L. Ludwig, K. H. Vousden, and A. M. Weissman.** 2000. Mdm2 is a RING finger-dependent ubiquitin protein ligase for itself and p53. J. Biol. Chem. **275:**8945–8951.
14. **Fang, S., K. L. Lorick, J. P. Jensen, and A. M. Weissman.** 2003. RING finger ubiquitin protein ligases: implications for tumorigenesis, metastasis and for molecular targets in cancer. Semin. Cancer Biol. **13:**5–14.
15. **Fusaro, G., P. Dasgupta, S. Rastogi, B. Joshi, and S. Chellappan.** 2003. Prohibitin induces the transcriptional activity of p53 and is exported from the nucleus upon apoptotic signaling. J. Biol. Chem. **278:**47853–47861.
16. **Itami, T., M. Maeda, M. Kondo, and Y. Takahashi.** 1999. Primary culture of lymphoid organ cells and haemocytes of kuruma shrimp, *Penaeus japonicus.* Methods Cell Sci. **21:**237–244.
17. **Jensen, M. R., and K. Helin.** 2004. OVCA1: emerging as a bona fide tumor suppressor. Genes Dev. **18:**245–248.
18. **Joazeiro, C. A., and A. M. Weissman.** 2000. RING finger proteins: mediators of ubiquitin ligase activity. Cell **102:**549–552.
19. **Joazeiro, C. A., S. S. Wing, H. Huang, J. D. Leverson, T. Hunter, and Y. C. Liu.** 1999. The tyrosine kinase negative regulator c-Cbl as a RING-type, E2-dependent ubiquitin-protein ligase. Science **286:**309–312.
20. **Khadijah, S., S. Y. Neo, M. S. Hossain, L. D. Miller, S. Mathavan, and J. Kwang.** 2003. Identification of white spot syndrome virus latency-related genes in specific-pathogen-free shrimps by use of a microarray. J. Virol. **77:**10162–10167.
21. **Kus, B. M., C. E. Caldon, R. Andorn-Broza, and A. M. Edwards.** 2004. Functional interaction of 13 yeast SCF complexes with a set of yeast E2 enzymes in vitro. Proteins **54:**455–467.
22. **Li, M., C. L. Brooks, F. Wu-Baer, D. Chen, R. Baer, and W. Gu.** 2003. Mono- versus polyubiquitination: differential control of p53 fate by Mdm2. Science **302:**1972–1975.
23. **Lightner, D. V.** 1996. A handbook of shrimp pathology and diagnostic procedures for diseases of cultured penaeid shrimp. World Aquaculture Society, Baton Rouge, La.
24. **Liu, Y. C.** 2004. Ubiquitin ligases and the immune response. Annu. Rev. Immunol. **22:**81–127.
25. **Lomonte, P., K. F. Sullivan, and R. D. Everett.** 2001. Degradation of nucleosome-associated centromeric histone H3-like protein CENP-A induced by herpes simplex virus type 1 protein ICP0. J. Biol. Chem. **276:**5829–5835.
26. **Notredame, C., D. G. Higgins, and J. Heringa.** 2000. T-Coffee: a novel method for fast and accurate multiple sequence alignment. J. Mol. Biol. **302:**205–217.
27. **Parkinson, J., S. P. Lees-Miller, and R. D. Everett.** 1999. Herpes simplex virus type 1 immediate-early protein vmw110 induces the proteasome-dependent degradation of the catalytic subunit of DNA-dependent protein kinase. J. Virol. **73:**650–657.
28. **Podgorski, I., and B. F. Sloane.** 2003. Cathepsin B and its role(s) in cancer progression. Biochem. Soc. Symp. **2003:**263–276.
29. **Saurin, A. J., K. L. Borden, M. N. Boddy, and P. S. Freemont.** 1996. Does this have a familiar RING? Trends Biochem. Sci. **21:**208–214.
30. **Schultz, D. C., L. Vanderveer, D. B. Berman, T. C. Hamilton, A. J. Wong, and A. K. Godwin.** 1996. Identification of two candidate tumor suppressor genes on chromosome 17p13.3. Cancer Res. **56:**1997–2002.
31. **Shih, W. L., H. W. Hsu, M. H. Liao, L. H. Lee, and H. J. Liu.** 2004. Avian reovirus σC protein induces apoptosis in cultured cells. Virology **321:**65–74.
32. **Sloane, B. F., S. Yan, I. Podgorski, B. E. Linebaugh, M. L. Cher, J. Mai, D. Cavallo-Medved, M. Sameni, J. Dosescu, and K. Moin.** 2005. Cathepsin B and tumor proteolysis: contribution of the tumor microenvironment. Semin. Cancer Biol. **15:**149–157.
33. **Sun, W., H. E. Khoo, and C. H. Tan.** 2005. Adenosine induced apoptosis in BHK cells via P1 receptors and equilibrative nucleoside transporters. J. Biochem. Mol. Biol. **38:**314–319.
34. **Thomas, M., D. Pim, and L. Banks.** 1999. The role of the E6-p53 interaction in the molecular pathogenesis of HPV. Oncogene **18:**7690–7700.
35. **Tsai, M. F., C. F. Lo, M. C. van Hulten, H. F. Tzeng, C. M. Chou, C. J. Huang, C. H. Wang, J. Y. Lin, J. M. Vlak, and G. H. Kou.** 2000. Transcriptional analysis of the ribonucleotide reductase genes of shrimp white spot syndrome virus. Virology **277:**92–99.
36. **Udawatte, C., and H. Ripps.** 2005. The spread of apoptosis through gap-junctional channels in BHK cells transfected with Cx32. Apoptosis **10:**1019–1029.
37. **van Hulten, M. C., J. Witteveldt, S. Peters, N. Kloosterboer, R. Tarchini, M. Fiers, H. Sandbrink, R. K. Lankhorst, and J. M. Vlak.** 2001. The white spot syndrome virus DNA genome sequence. Virology **286:**7–22.
38. **Vaux, D. L., and J. Silke.** 2005. IAPs, RINGs and ubiquitylation. Nat. Rev. Mol. Cell Biol. **6:**287–297.
39. **Wang, C. H., H. N. Yang, C. Y. Tang, C. H. Lu, G. H. Kou, and C. F. Lo.** 2000. Ultrastructure of white spot syndrome virus development in primary lymphoid organ cell cultures. Dis. Aquat. Organ. **41:**91–104.
40. **Wang, S., N. Nath, G. Fusaro, and S. Chellappan.** 1999. Rb and prohibitin target distinct regions of E2F1 for repression and respond to different upstream signals. Mol. Cell. Biol. **19:**7447–7460.
41. **Wang, Z., H. K. Chua, A. A. Gusti, F. He, B. Fenner, I. Manopo, H. Wang, and J. Kwang.** 2005. RING-H2 protein WSSV249 from white spot syndrome virus sequesters a shrimp ubiquitin-conjugating enzyme, PvUbc, for viral pathogenesis. J. Virol. **79:**8764–8772.
42. **Wang, Z., L. Hu, G. Yi, H. Xu, Y. Qi, and L. Yao.** 2004. ORF390 of white spot syndrome virus genome is identified as a novel anti-apoptosis gene. Biochem. Biophys. Res. Commun. **325:**899–907.
43. **Yang, F., J. He, X. Lin, Q. Li, D. Pan, X. Zhang, and X. Xu.** 2001. Complete genome sequence of the shrimp white spot bacilliform virus. J. Virol. **75:**11811–11820.
44. **Yang, Y., C. C. Li, and A. M. Weissman.** 2004. Regulating the p53 system through ubiquitination. Oncogene **23:**2096–2106.
45. **Yang, Y., and X. Yu.** 2003. Regulation of apoptosis: the ubiquitous way. FASEB J. **17:**790–799.
46. **Zheng, N., P. Wang, P. D. Jeffrey, and N. P. Pavletich.** 2000. Structure of a c-Cbl-UbcH7 complex: RING domain function in ubiquitin-protein ligases. Cell **102:**533–539.